Chemical Science

ROYAL SOCIETY OF CHEMISTRY

EDGE ARTICLE

View Article Online
View Journal | View Issue



Cite this: *Chem. Sci.*, 2021, **12**, 10883

All publication charges for this article have been paid for by the Royal Society of Chemistry

# Borane-catalyzed selective dihydrosilylation of terminal alkynes: reaction development and mechanistic insight†

Guoqiang Wang, ‡ Xiaoshi Su,‡ Liuzhou Gao,‡ Xueting Liu, Guoao Li and Shuhua Li *

Received 21st May 2021
Accepted 13th July 2021

DOI: 10.1039/d1sc02769g

rsc.li/chemical-science

Here, we describe simple $B(C_6F_5)_3$-catalyzed mono- and dihydrosilylation reactions of terminal alkynes by using a silane-tuned chemoselectivity strategy, affording vinylsilanes and unsymmetrical geminal bis(silanes). This strategy is applicable to the dihydrosilylation of both aliphatic and aryl terminal alkynes with different silane combinations. Gram-scale synthesis and conducting the reaction without the exclusion of air and moisture demonstrate the practicality of this methodology. The synthetic utility of the resulting products was further highlighted by the structural diversification of geminal bis(silanes) through transforming the secondary silane into other silyl groups. Comprehensive theoretical calculations combined with kinetical isotope labeling studies have shown that a prominent kinetic differentiation between the hydrosilylation of alkynes and vinylsilane is responsible for the chemoselective construction of unsymmetrical 1,1-bis(silanes).



## Introduction

Organosilanes have a multitude of applications in a variety of fields, ranging from organic synthesis to functional materials and pharmaceutical sciences.[1] Geminal bis(silanes) are particularly attractive due to their versatile synthetic utilities, and valuable structural and conformational properties.[2,3] However, the scarcity of practical protocols for their synthesis limits their structural diversity and their further synthetic utilities. Previous strategies for the synthesis of geminal bis(silanes) are mainly based on prefunctionalized precursors, such as *retro*-[1,4]-Brook rearrangement of 3-silyl allyloxy-silanes,[3a,b,d] insertion of benzylic carbenes into disilanes,[4] and double C–Si coupling of geminal dibromides.[5]

Synthesis of geminal bis(silanes) through dihydrosilylation of alkynes is an ideal way due to the high step- and atom-economy. Recently, several research groups have reported dihydrosilylation reaction of alkynes through transition-metal catalysis. For example, Lu's group and Zhu's group reported the catalytic 1,1-dihydrosilylation of terminal aliphatic alkynes with Co- and Fe-catalysts, affording symmetrical 1,1-bis(silanes), respectively (Scheme 1a).[6a,7] Besides, Cui's group also reported the dihydrosilylation of internal alkynes with rare-earth ate complexes, providing access to 1,1-di- or 1,1,1-trisilylated products.[8] More importantly, Lu and co-workers elegantly developed sequential catalysis with a combination of two Co-catalysts ($CoBr_2$, Xantphos and $CoBr_2$, OIP (OIP = oxazoline-iminopyridine)) to access unsymmetrical 1,1-bis(silanes) with aliphatic terminal alkynes (Scheme 1b).[6b] Although significant

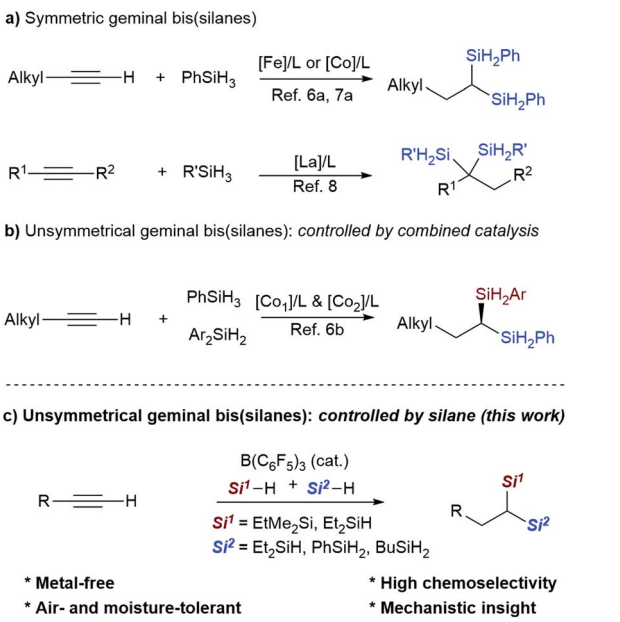


Scheme 1 Catalytic dihydrosilylation of alkynes. $R^1$ = alkyl; $R^2$ = aryl, alkyl or silyl group; R = alkyl or aryl.

*Institute of Theoretical and Computational Chemistry, School of Chemistry and Chemical Engineering, Nanjing University, Nanjing 210023, China. E-mail: shuhua@nju.edu.cn*

† Electronic supplementary information (ESI) available: Experimental details, characterization, and computational data. See DOI: 10.1039/d1sc02769g

‡ These authors contributed equally to this work.

advances have been achieved, currently available synthetic protocols are mainly applicable to terminal aliphatic alkynes or internal alkynes. The synthesis of 1,1-bis(silanes) with arylacetylenes is less reported. Scope investigation on Fe-catalyzed dihydrosilylation of terminal alkynes has shown that the reaction of 1-arylacetylene with hydrosilane only affords the monohydrosilylated product due to the steric effect.[7a,9]

Recently, the combination of commercially available tris(pentafluoro) borane ($B(C_6F_5)_3$)[10,11] and hydrosilanes (Si–H) has emerged as a highly versatile catalytic system for the hydrosilylation, silylation and selective defunctionalization of organic molecules to valuable intermediates,[12–15] providing a powerful alternative to the classical transition-metal catalysis. It should be noted that Gevorgyan's group has previously disclosed $B(C_6F_5)_3$-catalyzed hydrosilylation of alkenes about twenty years ago,[13c] but the catalytic hydro- or dihydrosilylation of terminal alkynes with the versatile $B(C_6F_5)_3$/Si–H system remains unknown. We herein report the development of a metal-free strategy for the selective dihydrosilylation of aliphatic or aryl-terminal alkynes with $B(C_6F_5)_3$ as the catalyst (Scheme 1c). This method allows the direct construction of unsymmetrical geminal bis(silanes) with a quaternary and a secondary silyl group, in which the Si–H bonds can be readily converted to other silyl groups. Mechanistic studies reveal that tertiary silanes (like $EtMe_2SiH$) favor the hydrosilylation of alkynes (1st hydrosilylation) while primary hydrosilanes (such as $PhSiH_3$ and $BuSiH_3$) favor the hydrosilylation of vinylsilane (2nd hydrosilylation).

## Results and discussion

### Reaction development

Although the realization of this strategy could provide a conceptually different approach for the synthesis of 1,1-bis(silanes), several possible problems should be overcome: first, hydrosilylation of alkynes generally yields alkenyl silanes, which are difficult for further hydrosilylation owing to the steric effect.[7a,9] Second, the control of chemoselectivity in the presence of two different hydrosilanes is also problematic (Scheme 2a). Third, the rapid and irreversible 1,1-carboboration reaction between a terminal alkyne and $B(C_6F_5)_3$ may lead to catalyst deterioration (Scheme 2b).[16,17] As a result, despite the broad application of $B(C_6F_5)_3$ in hydrosilylation reactions, its capability in the dihydrosilylation of alkynes has, to our knowledge, not been demonstrated.

We first examined the reaction conditions for catalytic monohydrosilylation of a terminal alkyne (Scheme 3a). At room temperature, the hydrosilylation of phenylacetylene **1a** using $B(C_6F_5)_3$/$EtMe_2SiH$ combination only affords *Z*-vinylsilane **3aa** in 31% yield.[18] This may probably be attributed to the occurrence of 1,1-carboboration reaction between phenylacetylene and $B(C_6F_5)_3$.[16,17] From a mechanistic point of view, the hydrosilylation pathway, involving a concerted three-molecular Si-centered displacement of a boron-coordinated hydride by the alkyne transition state ($S_{N^2}$@Si),[13,19] requires more entropy-cost than the two-molecular transition state toward the carboboration pathway. Therefore, we hypothesized that low temperatures might facilitate the entropy-disfavored hydrosilylation pathway. We were delighted to find that the yield was significantly improved from 58% to 84% when lowering the temperature from 5 to −40 °C. Then, the effect of hydrosilylation reagent was examined in the presence of 5 mol% of $B(C_6F_5)_3$ at −40 °C. Other hydrosilanes, including tertiary, secondary, and primary silanes, were not as effective as $EtMe_2SiH$ for monohydrosilylation of phenylacetylene (see Table S1† in the ESI for optimization details). It is worth noting that with secondary hydrosilane $Et_2SiH_2$, *Z*-vinyl silane was formed in 55% yield but accompanied by 25% yield of dihydrosilylated product. These results indicate that low temperature and suitable hydrosilanes are necessary to synthesize vinylsilane from terminal alkynes using $B(C_6F_5)_3$ as the catalyst. In addition to phenylacetylene, the reactivity of aliphatic terminal alkynes and internal alkynes was also investigated for the $B(C_6F_5)_3$-catalyzed

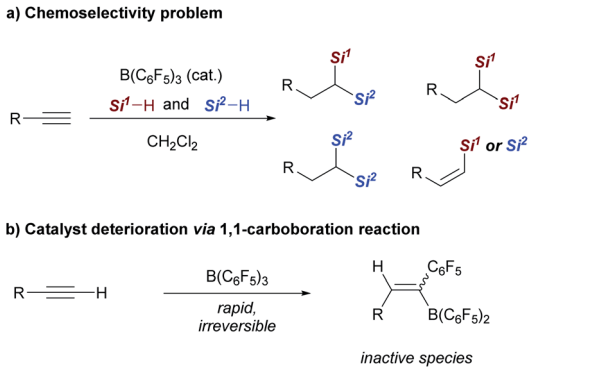


Scheme 2 Challenges in catalytic 1,1-dihydrosilylation of terminal alkynes with $B(C_6F_5)_3$.

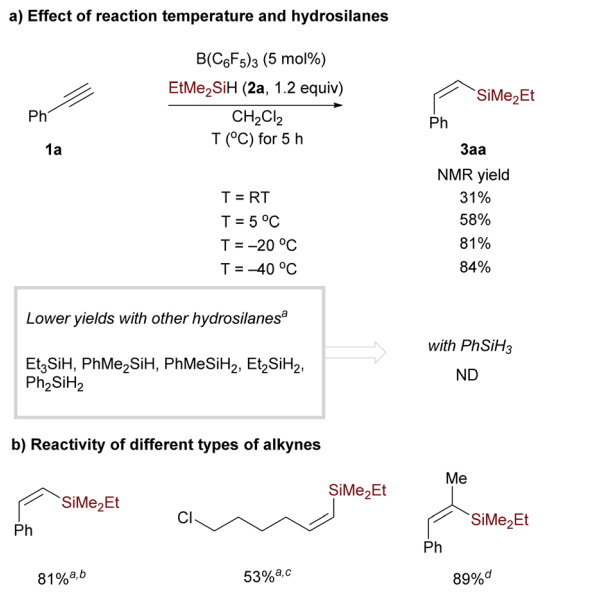


Scheme 3 Initial investigation on the monohydrosilylation of terminal alkynes. [a]Performed at −40 °C. [b]With 5 mol% $B(C_6F_5)_3$. [c]With 10 mol% $B(C_6F_5)_3$. [d]In 9 mmol scale, performed at room temperature with 0.25 mol% $B(C_6F_5)_3$. ND = not detected.

Table 1 Optimization of the dihydrosilylation reaction of alkynes[a]

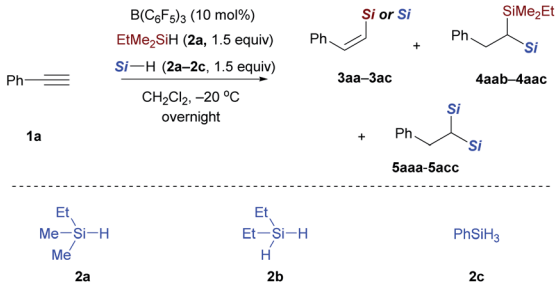


| Entry | Si–H combinations | 3 | 4 | 5 |
|---|---|---|---|---|
| 1[b,c] | **2a** | 76% | — | <5% |
| 2[c] | **2a** | 68% | — | 29% |
| 3 | **2a**/**2b** = 1 : 1 | ND | 66% | 34% |
| 4 | **2a**/**2c** = 1 : 1 | ND | >95% (92%) | ND |
| 5[d] | **2a**/**2c** = 1 : 1 | ND | >95% | ND |

[a] Reaction conditions: **1a** (0.4 mmol), $EtMe_2SiH$ (**2a**, 0.60 mmol), Si–H (**2a–2c**, 0.60 mmol), $B(C_6F_5)_3$ (0.04 mmol), in dichloromethane (1.0 mL). Yields were determined by NMR analysis; isolated yield in parentheses. [b] 5 mol% $B(C_6F_5)_3$. [c] With 3.0 equiv. of **2a**. [d] At −40 °C.

monohydrosilylation reaction. As shown in Scheme 3b, this method is applicable to both terminal and internal alkynes. It should be noted that the hydrosilylation of 1-phenylpropyne exhibits excellent regioselectivity and efficiency, the corresponding *Z*-vinylsilane could be prepared in 89% yield (9 mmol scale) with only 0.25 mol% of $B(C_6F_5)_3$.

After the monohydrosilylation reaction conditions were established, we then explored the dihydrosilylation of alkynes (Table 1). Using $EtMe_2SiH$ as the sole hydrosilane, only traces of dihydrosilylated product **5aaa** were observed, and most of the monohydrosilylated product **3aa** (76% NMR yield) was left unreacted at −20 °C in the presence of 5 mol% of $B(C_6F_5)_3$ (entry 1). Further increasing the catalyst loading from 5 mol% to 10 mol% did not significantly improve the yield of **5aaa** (entry 2). Replacing $EtMe_2SiH$ by an equimolar mixture of $EtMe_2SiH$ and $Et_2SiH_2$, unsymmetrical geminal bis(silane) **4aab** was formed in 66% yield (entry 3), but accompanied by 34% yield of symmetrical 1,1-bis(silane) **5abb** (dihydrosilylated by $Et_2SiH_2$). When a combination of $EtMe_2SiH$ and $PhSiH_3$ was used, phenylacetylene underwent two sequential hydrosilylation reactions to give the corresponding unsymmetrical 1,1-bis(silane) **4aac** in 92% isolated yield (entry 4).[20] Reaction performed overnight at a lower temperature (−40 °C) did not decrease the yield of the desired product (entry 5).

## Examination of substrate scope

We then evaluated a series of terminal alkynes to probe the substrate scope (Scheme 4). Substrates with electron-withdrawing (**1b–1i**) or electron-donating (**1j–1n**) substituents underwent dihydrosilylation with good efficiency, transforming the terminal alkyne into the corresponding 1,1-bis(silanes) in reaction with an equimolar mixture of $EtMe_2SiH$ and $PhSiH_3$.

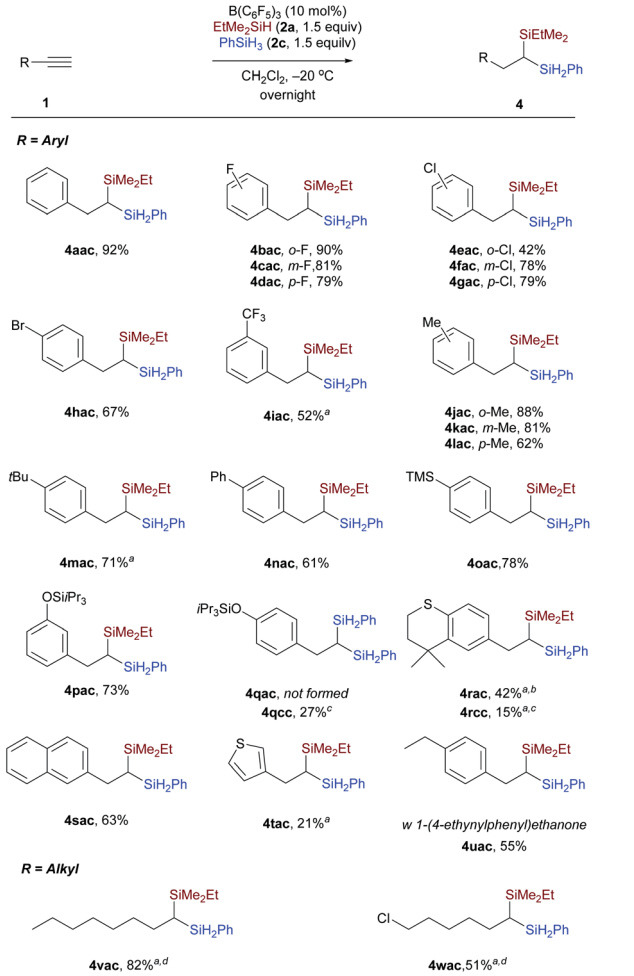


Scheme 4 Substrate scope. Isolated yields after flash chromatography. [a]20 mol% $B(C_6F_5)_3$ was used. [b]$PhSiH_3$ was added in 5 hours delay after the initial $EtMe_2SiH$ addition. [c]Dihydrosilylated by $PhSiH_3$. [d]Stirred at −40 °C for 5 h, and then 24 h at room temperature.

Functional groups, including halides (F, Cl, Br, **1b–1h**), trifluoromethyl ($CF_3$, **1i**), and trimethylsilyl (TMS, **1o**) were tolerated. 3-Triisopropylsilyl-*O*-substituted phenylacetylene was selectively dihydrosilylated to yield unsymmetrical 1,1-bis(silane) **4pac**. The reaction of 1-ethynyl-4-[[tris(1-methylethyl)silyl]oxy]benzene with $EtMe_2SiH$ and $PhSiH_3$ under standard conditions only affords the symmetrical geminal silane **4qcc** in 27% (dihydrosilylated by $PhSiH_3$). This is probably due to the fact that the kinetics or reaction mechanism of the substrate with strong electron-donating substituents is different from phenylacetylenes with weak electron-donating substituents. Similarly, alkyne **1r** with a cyclic thioether also did not afford the corresponding unsymmetrical bis(silane) **4rac** according to the general procedure, but afforded **4rcc** in 15% yield (dihydrosilylated by $PhSiH_3$). The unsymmetrical 1,1-bis(silane) **4rac** could be obtained in 42% yield by slightly changing the reaction conditions. Aside from phenylacetylene derivatives, a β-naphthyl and a thiophene-3-yl as in **1s** and **1t** were also compatible with the reaction conditions, leading to products **4sac** and **4tac**, respectively, with moderate and slightly lower yields. However,

functional groups including ether, ester, aldehyde, ketone, carboxylic acid, and amide were not tolerated because of the high reduction or defunctionalization ability of $B(C_6F_5)_3$/hydrosilane combinations. For example, when 1-(4-ethynylphenyl)ethanone was subjected to the mixture of $B(C_6F_5)_3$ and hydrosilane at −20 °C, we could only isolate the decarbonylated 1,1-bis(silane) **4uac**. In addition to phenylacetylenes, terminal alkynes with aliphatic side chains were also viable (Scheme 4, bottom). Oct-1-yne **1v** and 6-chlorohex-1-yne **1w** could be dihydrosilylated to give the related 1,1-bis(silanes) **4vac** and **4wac** by simply stirring the reaction mixture at −40 °C for 5 hours and then at room temperature for an additional 24 hours. The reactivity difference between aryl and aliphatic terminal alkynes can be rationalized by the stability of different types of carbon cations involved. However, the reaction of the internal alkyne, 1-phenyl-1-propyne, only affords the monohydrosilylated compound as the major product. Different from Fe-catalyzed dihydrosilylation of terminal alkynes, in which only aliphatic terminal alkynes can be transformed into the corresponding symmetrical geminal bis(silanes) with primary silanes,[7a] our approach is applicable to both aryl and alkyl-substituted terminal alkynes.

Then, the reactivity observed in Table 1 intrigued us to construct geminal bis(silanes) with other hydrosilane combinations. As shown in Scheme 5, using $Et_2SiH_2$ as the sole silane, a symmetrical geminal bis(silane) **5abb** with two tertiary silane moieties was obtained in excellent yield. Moreover, the reaction of $Et_2SiH_2$/$PhSiH_3$ and $EtMe_2SiH_2$/$BuSiH_3$ combination with phenylacetylene also worked effectively and selectively to give the unsymmetrical 1,1-bis(silane) **4abc** and **4aad** in 62% and 81% yield, respectively. To further identify the silane effect in the second hydrosilylation step, we subjected **3aa** to the standard procedures with an equimolar mixture of $Et_2SiH_2$ and $PhSiH_3$, and detected the exclusive formation of **4aac** (Scheme 5, middle; selectively hydrosilylated by $PhSiH_3$). These results confirmed that the primary silane is more reactive than secondary and tertiary hydrosilanes in the second hydrosilylation step (vinylsilane hydrosilylation). This trend is consistent with the size of the hydrosilanes. Although the use of $EtMe_2SiH$ and $Et_2SiH_2$ combination gives a mixture of two different dihydrosilylation products (*cf.* Table 1, entry 3), the unsymmetrical 1,1-bis(silane) **4aab** can be obtained in 81% yield by simply adding $Et_2SiH_2$ in 5 hours delay after the initial $EtMe_2SiH$ addition (Scheme 5, bottom).

To demonstrate the practicality of this protocol in preparative organic synthesis, a gram-scale reaction was conducted. As shown in Scheme 6a, in the presence of 10 mol% $B(C_6F_5)_3$, 2.7 grams of **4aac** could be prepared with phenylacetylene in 90% yield. Moreover, the reaction could be conducted with all reagents handled in the open atmosphere without exclusion of air and moisture; the yield was 90% in 1 mmol scale (Scheme 6b).[21] The two Si–H bonds in the secondary silane of **4aac** can be readily converted to Si–O (**6** and **7**) and Si–F bonds (**8**) (Scheme 6c), enriching the structural diversity of the geminal bis(silanes).

## Mechanism of borane-catalyzed dihydrosilylation of terminal alkynes

**Comparison of the influence of hydrosilanes on alkyne hydrosilylation and vinylsilane hydrosilylation.** The experimental results collected in Scheme 7 show that for the hydrosilylation of phenylacetylene, replacement of the ethyl group in $EtMe_2SiH$ by phenyl ($PhMe_2SiH$) leads to a reduced yield of vinylsilane (84% *versus* 46%). Hydrosilylation of **1a** with $Et_2SiH_2$ exhibits higher reactivity than $PhMeSiH_2$, albeit accompanied by the formation of symmetric geminal bis(silane); both $Ph_2SiH_2$ and $PhSiH_3$ are inactive for the hydrosilylation of

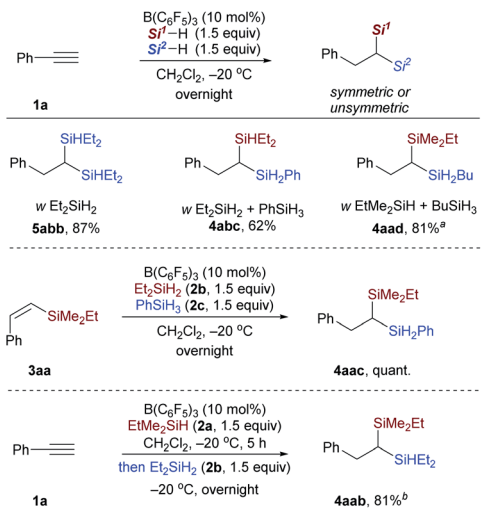


Scheme 5 Reactivity of other hydrosilane combinations. Isolated yields after flash chromatography. [a]A slight amount of symmetric geminal bis(silane) was detected (unsymmetric : symmetric > 10 : 1). [b]$Et_2SiH_2$ was added in 5 hours delay after the initial $EtMe_2SiH$ addition.

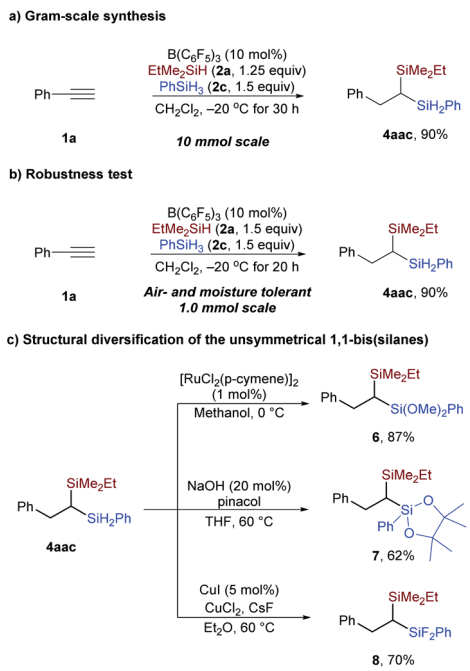


Scheme 6 Reaction practicality and product transformation.

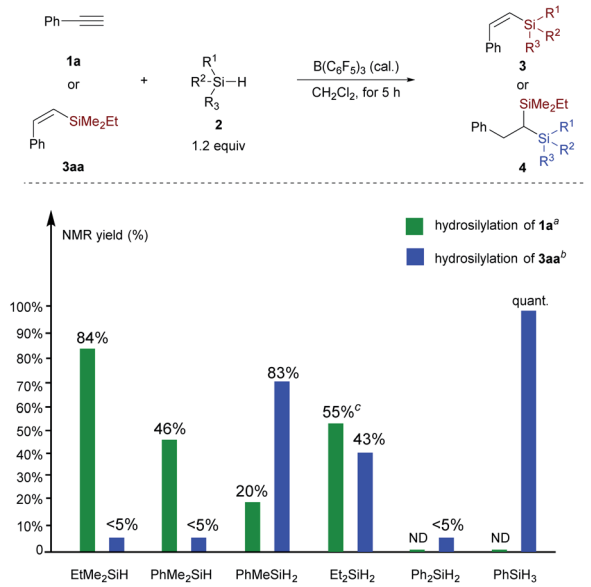


Scheme 7 Comparison of the influence of hydrosilanes on alkyne hydrosilylation and vinylsilane hydrosilylation. [a]Hydrosilylation of phenylacetylene **1a**: performed at −40 °C with 10 mol% $B(C_6F_5)_3$ in 0.4 mmol scale. [b]Hydrosilylation of vinylsilane **3aa**: performed at −20 °C with 5 mol% $B(C_6F_5)_3$ in 0.2 mmol scale. [c]Dihydrosilylated product formed with $Et_2SiH_2$, see Table S1† for details.

phenylacetylene. These results suggest that hydrosilylation of phenylacetylene is controlled by the electronic effect, and the observed reactivity order is consistent with the electron-donating ability (Me > Ph > H) of hydrosilanes as measured by Mayr *et al.*[22] However, the reactivity of vinylsilane hydrosilylation is significantly different from alkyne hydrosilylation. Tertiary silane is less reactive than secondary and primary hydrosilane. Replacement of the two ethyl groups in $Et_2SiH_2$ by phenyl groups leads to little reactivity. Besides, we also performed the hydrosilylation reaction of **3aa** in the presence of two secondary hydrosilanes $Et_2SiH_2$ (**2b**) and $PhMeSiH_2$ (**2e**). The reaction rate of **3aa** with $PhMeSiH_2$ is faster than that of $Et_2SiH_2$ (**4aab**/**4aae** = 1 : 3.5, see Scheme S2 and Fig. S3† for details). This result confirms the importance of the steric effect in the hydrosilylation of vinylsilane. However, when performing the hydrosilylation reaction of **3aa** in the presence of two primary silanes $PhSiH_3$ and $BuSiH_3$, alkylsilane $BuSiH_3$ shows higher reactivity than $PhSiH_3$; and the corresponding geminal bis(silanes) were obtained in 2.4 : 1 ratio (see Scheme S2 and Fig. S4† for details). To conclude from these control experiments, we can get the reactivity order for the hydrosilylation of vinylation: $EtMe_2SiH < Et_2SiH_2 < PhMeSiH_2 < PhSiH_3 < BuSiH_3$. These observations suggest that hydrosilylation of vinylsilane mainly depends on the steric effect, but electronic effects also play a role in the hydrosilylation of vinylsilane with primary hydrosilanes.

**DFT calculations on the full catalytic cycle.** Computational studies with the M06-2X functional[23] were undertaken to gain more mechanistic insight. The solvent effect was treated with the PCM[24] solvation model and with dichloromethane as the solvent in structural optimization and single-point energy

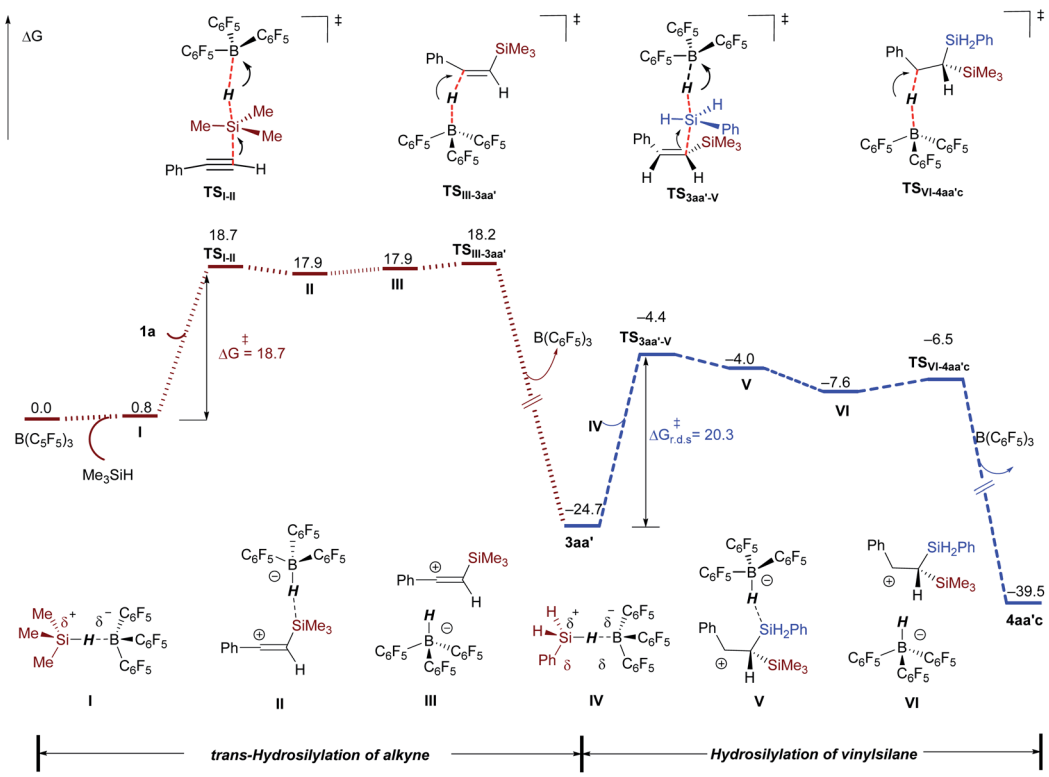


Fig. 1 Gibbs free energy profile (298.15 K) for the $B(C_6F_5)_3$-catalyzed dihydrosilylation of alkyne (in kcal $mol^{-1}$). Performed at the M06-2X/cc-pVTZ/(PCM, $CH_2Cl_2$)//M06-2X/6-311G(d,p)/(PCM, $CH_2Cl_2$) level of theory. r.d.s = rate-determining step.

calculations (see ESI† for computational details).[25] The dihydrosilylation of phenylacetylene **1a** with $Me_3SiH/PhSiH_3$ combination was selected as the model reaction. The complete free energy profile is displayed in Fig. 1 (see Fig. S6† for optimized structures). The sequential dihydrosilylation of alkyne proceeds through a classical Piers–Oestreich-type mechanism,[13,19] wherein substrate **1a** (alkyne hydrosilylation, in brown line) or *in situ* formed vinylsilane **3aa′** (vinylsilane hydrosilylation, in blue line) attacks the Si center in the $B(C_6F_5)_3$-hydrosilane η1-adduct **I** or **IV** (*via* $\mathbf{TS_{I\text{-}II}}$ or $\mathbf{TS_{3aa'\text{-}V}}$) to form the ion-pair species **II** or **V**. The barrier for Si–H bond cleavage in adduct **I** with alkyne (*via* $\mathbf{TS_{I\text{-}II}}$) is computed to be 18.7 kcal $mol^{-1}$, and the Si–H bond cleavage in adduct **IV** with vinylsilane as a nucleophile ($\mathbf{TS_{3aa'\text{-}V}}$) requires a slightly higher activation barrier of 20.3 kcal $mol^{-1}$. Both ion-pair species **II** and **IV** are readily reorganized to their isomers **III** and **VI**,[19] in which the anion B–H is oriented towards the carbon cation center (vinyl cation or β-silylcarbenium ion). Then, hydride transfer from the borohydride to the electrophilic carbon atom in the ion-pair **III** (*via* $\mathbf{TS_{III\text{-}3aa'}}$, $\Delta G^{\ddagger} = 18.2$ kcal $mol^{-1}$) or **VI** (*via* $\mathbf{TS_{VI\text{-}4aa'c}}$, $\Delta G^{\ddagger} = 18.2$ kcal $mol^{-1}$) generates the *trans*-hydrosilylation product **3aa′** or dihydrosilylated product **4aa′c**, respectively. In addition, the *cis*-hydrosilylation pathway involving hydride transfer from borohydride to the vinyl cation at the same side of the silyl group (leading to *E*-**3aa′**) was also considered. This process is less kinetically favorable than the *trans*-hydrosilylation pathway ($\Delta G^{\ddagger} = 24.1$ *versus* 18.2 kcal $mol^{-1}$, see Fig. S7†). Along the whole dihydrosilylation pathway, nucleophilic attack of vinylsilane **3aa′** at the Si center of the $B(C_6F_5)_3$-$PhSiH_3$ adduct **IV** ($\mathbf{TS_{3aa'\text{-}V}}$) with an activation barrier of 20.3 kcal $mol^{-1}$ is the rate-limiting step, which is consistent with the mild reaction conditions.

### Rationalization of the reactivity difference of hydrosilanes

Based on the reactivity difference observed in dihydrosilylation of terminal alkynes that depend on hydrosilanes, we then focused on gaining insights into the origin of chemoselectivity in this catalytic system.

**Hydrosilylation of terminal alkynes (1st hydrosilylation).** To compare the reactivity of silanes on the hydrosilylation of alkynes, we computed the energy barriers of the 1st hydrosilylation step (**I** → **II**) with representative hydrosilanes ($Me_3SiH$, $Me_2SiH_2$, and $PhSiH_3$). As shown in Fig. 2, the activation barrier for the secondary hydrosilane $Me_2SiH_2$ here is slightly higher than that with $Me_3SiH$ (19.4 *versus* 18.7 kcal $mol^{-1}$); but both of which are lower than the barrier of the carboboration reaction between $B(C_6F_5)_3$ and phenylacetylene **1a** (21.6 kcal $mol^{-1}$, see Fig. S8† in the ESI). With

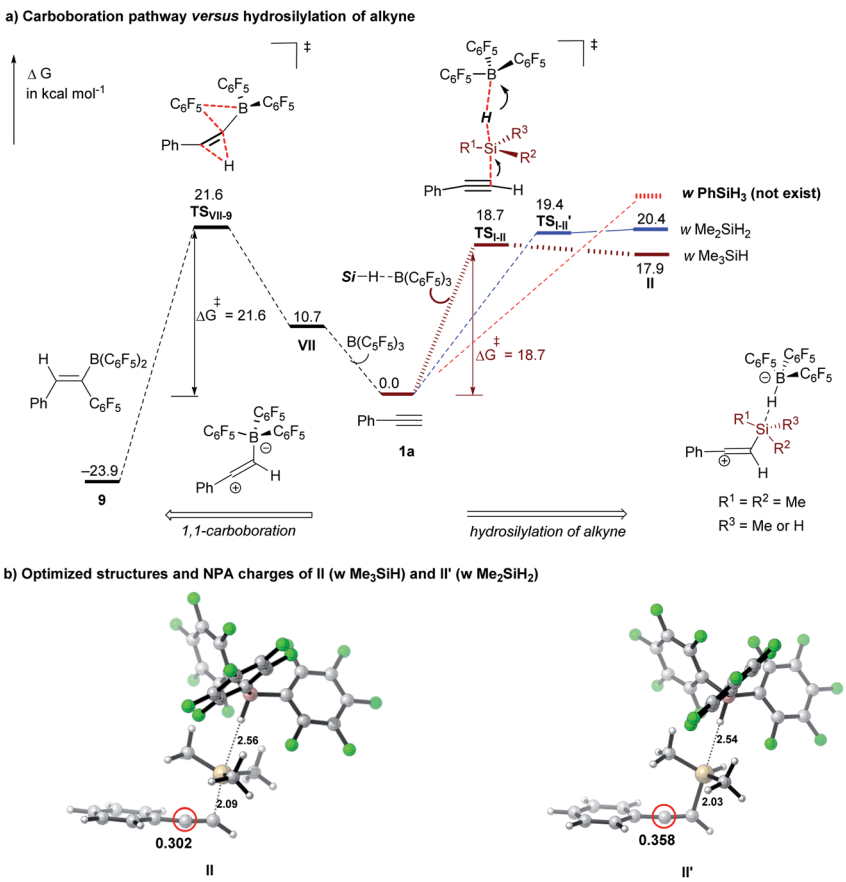


Fig. 2 (a) Comparison of the carboboration pathway and the $B(C_6F_5)_3$-catalyzed hydrosilylation of alkyne. Performed at the M06-2X/cc-pVTZ/(PCM, $CH_2Cl_2$)//M06-2X/6-311G(d,p)/(PCM, $CH_2Cl_2$) level of theory (energies are in kcal $mol^{-1}$); (b) optimized structures and NPA charges for ion-pair species **II** (with $Me_3SiH$) and **II′** (with $Me_2SiH_2$).

$PhSiH_3$, however, the related $S_{N^2}$@Si transition state could not be located after extensive endeavors (Fig. S10†). Our further calculations show that the resulting ion-pair intermediate doesn't exist as a minimum structure on the potential energy surface (Fig. 2, red dashed line). These results suggest that both $Me_3SiH$ and $Me_2SiH_2$ are suitable for the hydrosilylation of terminal alkynes, but the primary silane $PhSiH_3$ is not effective. NPA charge calculations reveal that the benzylic carbon of the ion-pair intermediate **II′** for $Me_2SiH_2$ (Fig. 2b, **II′**: 0.358*e*) is more positively charged than that in **II** (for $Me_3SiH$, **II**: 0.302*e*). These computational results also support that the hydrosilylation of the terminal alkyne is probably controlled by the electronic effect, being consistent with these experimental results.

To understand the origin of reactivity difference, we undertook NMR analysis on the hydrosilylation reactions of **1a** with $EtMe_2SiH$ or $Et_2SiH$ and $PhSiH_3$, respectively. The crude $^1H$ NMR spectra clearly show the formation of the hydrosilylation or dihydrosilylation product with $EtMe_2SiH$ or $Et_2SiH_2$ in the presence of 20 mol% $B(C_6F_5)_3$ (Fig. S1 in the ESI†). We were able to detect the characteristic peaks of $B(C_6F_5)_3$ (*i.e.*, 128.1, 144.0, 160.9 ppm) from the $^{19}F$ NMR spectra (Fig. S2 in the ESI†). However, only a trace amount of dihydrosilylated product was detected with $PhSiH_3$ as the silane source. The $^{19}F$ NMR spectrum of the reaction mixture of $PhSiH_3$, **1a** and 20 mol% of $B(C_6F_5)_3$ confirms the deterioration of $B(C_6F_5)_3$ in the case of $PhSiH_3$. We attribute this to the occurrence of the carboboration reaction of **1a** with $B(C_6F_5)_3$ or other unknown oligomerization or polymerization reactions (see Scheme S1† for Computational analysis). These results are in line with our theoretical calculations that both $EtMe_2SiH$ and $Et_2SiH_2$ are suitable silanes for the first hydrosilylation step.

**Hydrosilylation of vinylation (2nd hydrosilylation).** The choice of silane combinations has a significant influence on the dihydrosilylation of alkynes: (1) the use of $EtMe_2SiH$ as the sole silane mainly gave the monohydrosilylation product; (2) the use of $EtMe_2SiH/PhSiH_3$, or $Et_2SiH_2/PhSiH_3$, or $EtMe_2SiH/Et_2SiH_2$ combination could produce the corresponding unsymmetrical geminal bis(silanes), as shown in Table 1 and Scheme 5. Our calculations reveal that the experimentally observed reactivity is in good accordance with the computed activation barriers of the 2nd $S_{N^2}$@Si transition states (vinylsilane hydrosilylation, Fig. 3). As the size of hydrosilane increases, the Gibbs free energy barrier increases from 20.3 kcal $mol^{-1}$ with the primary silane $PhSiH_3$ to 22.5 kcal $mol^{-1}$ with the secondary silane $Me_2SiH_2$, and to 26.5 kcal $mol^{-1}$ with the tertiary silane $Me_3SiH$. In $\mathbf{TS_{3aa'a'}}$ (vinylsilane hydrosilylation with $Me_3SiH$), the trimethylsilyl (TMS) group in $Me_3SiH$ introduces large steric congestion around $B(C_6F_5)_3$ to destabilize the transition state.[26] This leads to increased distances between the reacting atoms in $\mathbf{TS_{3aa'a'}}$ ($d_{Si-H} = 2.12$ Å and $d_{Si-C} = 2.55$ Å) compared to those in $\mathbf{TS_{3ab'b'}}$ ($d_{Si-H} = 2.05$ Å and $d_{Si-C} = 2.28$ Å) and those in $\mathbf{TS_{3aa'\text{-}V}}$ ($d_{Si-H} = 1.88$ Å and $d_{Si-C} = 2.26$ Å). In addition, with $Me_2SiH_2$ as the substrate, we located another transition state ($\mathbf{TS_{3ab'b'\text{-}iso}}$) (an isomer of $\mathbf{TS_{3ab'b'}}$) with the silyl group rotated by 120°. This transition state has a higher activation barrier than $\mathbf{TS_{3ab'b'}}$ (24.3 *versus* 22.5 kcal $mol^{-1}$), indicating that the steric effect is a key factor in the 2nd hydrosilylation step.

**Kinetic isotope effect (KIE) determination for the hydrosilylation of the vinylsilane step.** To further gain insight into the rate-determining step, intermolecular KIE was determined from the initial reaction rates of two parallel reactions of vinylsilane **3aa** with $PhSiH_3$ and $PhSiD_3$ (Scheme 8 and Fig. S5†). An inverse secondary deuterium KIE ($k_H/k_D = 0.81$) was observed in the hydrosilylation reaction of vinylsilane in the presence of 2.25 mmol% of $B(C_6F_5)_3$ (Scheme 8a). KIE values of 1.4–1.9 have been reported for the hydrosilylation of carbonyl compounds and heterodehydrocoupling of phosphines and hydrosilanes.[13b,27] These values were interpreted in terms of hydride transfer.[28] To identify the origin of the observed kinetic isotope effect, KIE calculations using the theory of the Bigeleisen–Mayer equation[29] and the rigid-rotor harmonic oscillator approach[30] were conducted on the related transition states involved in the hydrosilylation of vinylsilane (see ESI† for Computational details).[31] As shown in Scheme 8b, our calculations indicate that the measured inverse secondary KIE is related to the $S_{N^2}$@Si transition state involving the displacement of hydride at the silicon atom with vinylsilane as the nucleophile ($\mathbf{TS_{3aa'\text{-}V}}$, $KIE_{comp} = 0.75$, Table S4†), rather than the hydride transfer step ($KIE_{comp} = 1.39$). The inverse secondary KIE may come from the hybridization change of the silicon center from tetravalent in $PhSiH_3$ to pentavalent in the transition state $\mathbf{TS_{3aa'\text{-}V}}$. With these computational and experimental results, we can conclude that the Si–H bond cleavage in adduct **IV** (*via* $\mathbf{TS_{3aa'\text{-}V}}$) featuring a pentavalent silicon species is involved in the rate-determining step.

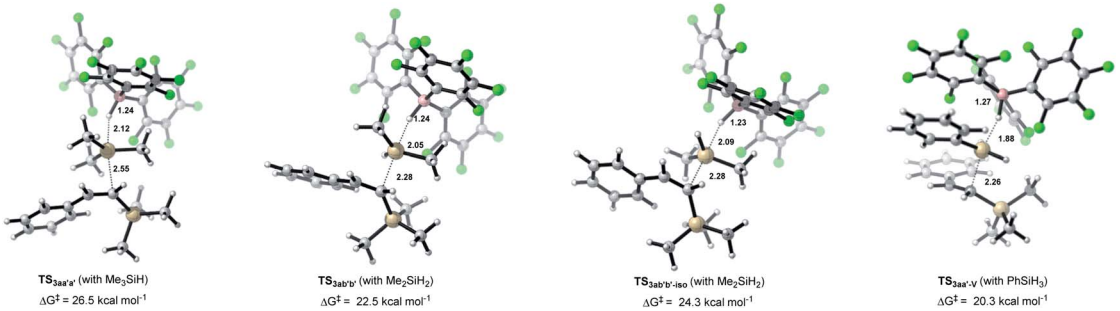


Fig. 3 Optimized geometries of Si–H cleavage transition states with vinylsilane as the nucleophile. Reaction barriers are given in kcal $mol^{-1}$. Color code: H, white; C, gray; B, pink; F, green; Si, brown.

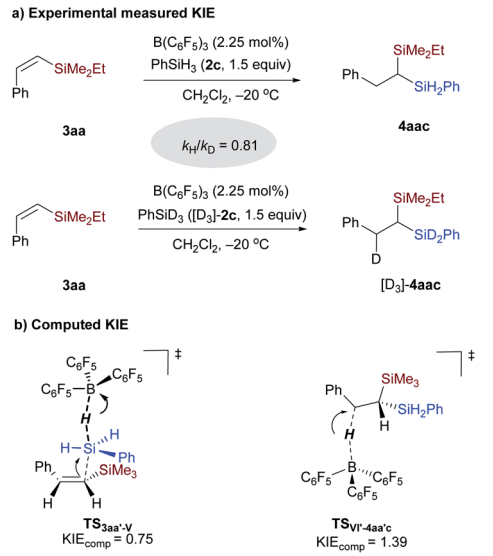


Scheme 8 Kinetic isotope effect determination for the borane-catalyzed hydrosilylation reaction of vinylsilane **3aa**.

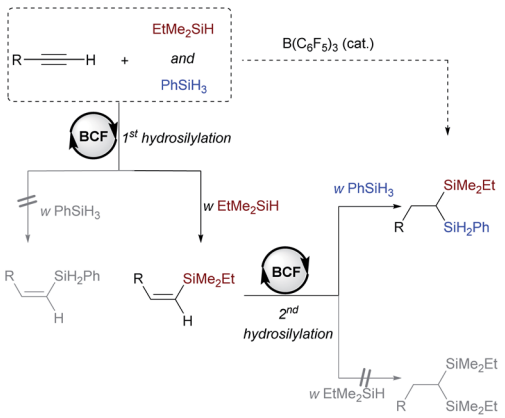


Scheme 9 Mechanistic proposal for borane-catalyzed dihydrosilylation of terminal alkynes giving rise to unsymmetrical geminal bis(silanes). BCF = $B(C_6F_5)_3$.

Based on the experimental and computational studies, we summarized the mechanistic details of the borane-catalyzed dihydrosilylation of alkynes in Scheme 9. The selective formation of unsymmetrical geminal bis(silanes) is a kinetically controlled process, in which the alkyne hydrosilylation can readily occur with $EtMe_2SiH$. In turn, the hydrosilylation of vinylsilane with primary silane is much more efficient than that with $EtMe_2SiH$. The high selectivity toward the unsymmetrical geminal bis(silane) rather than symmetrical products could be rationalized by a combination of steric and electronic effects.

## Conclusions

We have developed a borane-catalyzed selective dihydrosilylation reaction of terminal alkynes to obtain synthetic valuable unsymmetrical geminal bis(silanes), using a combination of a tertiary silane (or secondary silane) and primary silane. The method exhibits broad substrate scope and can be run in the presence of air and moisture. The resulting silane reagents can be readily functionalized through Si–H bond transformation, increasing the structural diversification of geminal bis(silanes). Combined theoretical calculations and experimental studies shed light on the mechanism, which can account for the high chemoselectivity toward unsymmetrical geminal bis(silanes). We expect our present work to stimulate future studies of boron/silane-related transformations as well as the synthetic utilities of unsymmetrical geminal bis(silane) products obtained through this protocol.

## Data availability

The datasets supporting this article have been uploaded as part of the ESI.†

## Author contributions

G. W., X. S., and L. G. performed the experiments. G. W. carried out the theoretical calculations. G. L. computed the KIE values. X. S. and X. L. characterized the compounds. G. W. and S. L. designed the project, analyzed the results and wrote the manuscript.

## Conflicts of interest

There are no conflicts to declare.

## Acknowledgements

G. W. and S. L. thank the National Natural Science Foundation of China (Grant Nos. 22073043, 21903043, 21833002, and 21673110), and the Fundamental Research Funds for the Central Universities (020514380243) for financial support. We thank Prof. Jing Ma and Prof. Xu Cheng for their helpful suggestion on the work. All theoretical calculations were performed on the High-Performance Computing Center (HPCC) of Nanjing University.

## Notes and references

1 *The Chemistry of Organic Silicon Compounds*, ed. Z. Rappoport and Y. Apeloig, Wiley, New York, 1998, vol. 2, p. 1687.
2 For a recent review on geminal bis(silanes), see: L. Gao, Y. Zhang and Z. Song, *Synlett*, 2013, **24**, 139–144.
3 For selected examples, see: (*a*) D. R. Williams, A. I. Morales-Ramos and C. M. Williams, *Org. Lett.*, 2006, **8**, 4393–4396; (*b*) Z. Yin, Z. Liu, Z. Huang, Y. Chu, Z. Chu, J. Hu, L. Gao and Z. Song, *Org. Lett.*, 2015, **17**, 1553–1556; (*c*) Z. Liu, X. Lin, N. Yang, Z. Su, C. Hu, P. Xiao, Y. He and Z. Song, *J. Am. Chem. Soc.*, 2016, **138**, 1877–1883; (*d*) Z. Chu, K. Wang, L. Gao and Z. Song, *Chem. Commun.*, 2017, **53**, 3078–3081; (*e*) Y. Zhang, Q. Guo, X. Sun, J. Lu, Y. Cao, Q. Pu, Z. Chu, L. Gao and Z. Song, *Angew. Chem., Int. Ed.*, 2018, **57**, 942–946.
4 Z. Liu, H. Tan, T. Fu, Y. Xia, D. Qiu, Y. Zhang and J. Wang, *J. Am. Chem. Soc.*, 2015, **137**, 12800–12803.

5 H. Hazrati and M. Oestreich, *Org. Lett.*, 2018, **20**, 5367–5369.
6 (*a*) Z. Cheng, S. Xing, J. Guo, B. Cheng, L.-F. Hu, X.-H. Zhang and Z. Lu, *Chin. J. Chem.*, 2019, **37**, 457–461; (*b*) J. Guo, H. Wang, S. Xing, X. Hong and Z. Lu, *Chem*, 2019, **5**, 881–895.
7 (*a*) M.-Y. Hu, J. Lian, W. Sun, T.-Z. Qiao and S.-F. Zhu, *J. Am. Chem. Soc.*, 2019, **141**, 4579–4583; (*b*) M.-Y. Hu, P. He, T.-Z. Qiao, W. Sun, W.-T. Li, J. Lian, J.-H. Li and S.-F. Zhu, *J. Am. Chem. Soc.*, 2020, **142**, 16894–16902.
8 W. Chen, H. Song, J. Li and C. Cui, *Angew. Chem., Int. Ed.*, 2020, **59**, 2365–2369.
9 (*a*) R. J. P. Corriu, M. Granier and G. F. Lanneau, *J. Organomet. Chem.*, 1998, **562**, 79–88; (*b*) P.-F. Fu, *J. Mol. Catal. A: Chem.*, 2006, **243**, 253–257.
10 For reviews on the chemistry of electron-deficient boron Lewis acids: (*a*) W. E. Piers and T. Chivers, *Chem. Soc. Rev.*, 1997, **26**, 345–354; (*b*) M.-A. Légaré, C. Pranckevicius and H. Braunschweig, *Chem. Rev.*, 2019, **119**, 8231–8261.
11 Application of $B(C_6F_5)_3$ in Frustrated Lewis Pair (FLP) chemistry, see: (*a*) G. C. Welch, R. R. San Juan, J. D. Masuda and D. W. Stephan, *Science*, 2006, **314**, 1124–1126; (*b*) P. A. Chase, G. C. Welch, T. Jurca and D. W. Stephan, *Angew. Chem., Int. Ed.*, 2007, **46**, 8050–8053; (*c*) G. C. Welch and D. W. Stephan, *J. Am. Chem. Soc.*, 2007, **129**, 1880–1881; (*d*) P. Spies, S. Schwendemann, S. Lange, G. Kehr, R. Fröhlich and G. Erker, *Angew. Chem., Int. Ed.*, 2008, **47**, 7543–7546.
12 For recent reviews, see: (*a*) D. Weber and M. R. Gagné, in *Organosilicon Chemistry: Novel Approaches and Reactions*, ed. T. Hiyama and M. Oestreich, Wiley-VCH, Weinheim, 2019, pp. 33–85; (*b*) M. Oestreich, J. Hermeke and J. Mohr, *Chem. Soc. Rev.*, 2015, **44**, 2202–2220; (*c*) W. Meng, X. Feng and H. Du, *Acc. Chem. Res.*, 2018, **51**, 191–201; (*d*) T. Hackel and N. A. McGrath, *Molecules*, 2019, **24**, 432; (*e*) H. Fang and M. Oestreich, *Chem. Sci.*, 2020, **11**, 12604–12615.
13 (*a*) D. J. Parks and W. E. Piers, *J. Am. Chem. Soc.*, 1996, **118**, 9440–9941; (*b*) D. J. Parks, J. M. Blackwell and W. E. Piers, *J. Org. Chem.*, 2000, **65**, 3090–3098; (*c*) M. Rubin, T. Schwier and V. Gevorgyan, *J. Org. Chem.*, 2002, **67**, 1936–1940; (*d*) S. Rendler and M. Oestreich, *Angew. Chem., Int. Ed.*, 2008, **47**, 5997–6000; (*e*) A. Y. Houghton, J. Hurmalainen, A. Mansikkamäki, W. E. Piers and H. M. Tuononen, *Nat. Chem.*, 2014, **6**, 983–988.
14 Selected examples of defunctionalization reactions with borane/silane combinations: (*a*) V. Gevorgyan, M. Rubin, J.-X. Liu and Y. Yamamoto, *J. Org. Chem.*, 2001, **66**, 1672–1675; (*b*) L. L. Adduci, T. A. Bender, J. A. Dabrowski and M. R. Gagné, *Nat. Chem.*, 2015, **7**, 576–581; (*c*) T. Mahdi and D. W. Stephan, *Angew. Chem., Int. Ed.*, 2015, **54**, 8511–8514; (*d*) J. Lowe, B. Bowers, Y. Seo and M. R. Gagné, *Angew. Chem., Int. Ed.*, 2020, **59**, 17297–17300.
15 For some recent transformations based on the borane/silane catalytic system, see: (*a*) N. Gandhamsetty, S. Joung, S.-W. Park, S. Park and S. Chang, *J. Am. Chem. Soc.*, 2014, **136**, 16780–16783; (*b*) C. K. Hazra, N. Gandhamsetty, S. Park and S. Chang, *Nat. Commun.*, 2016, **7**, 13431; (*c*) Y. Ma, B. Wang, L. Zhang and Z. Hou, *J. Am. Chem. Soc.*, 2016, **138**, 3663–3666; (*d*) Y. Ma, L. Zhang, Y. Luo, M. Nishiura and Z. Hou, *J. Am. Chem. Soc.*, 2017, **139**, 12434–12437; (*e*) Z.-Y. Zhang, Z.-Y. Liu, R.-T. Guo, Y.-Q. Zhao, X. Li and X.-C. Wang, *Angew. Chem., Int. Ed.*, 2017, **56**, 4028–4032; (*f*) C. K. Hazra, J. Jeong, H. Kim, M. H. Baik, S. Park and S. Chang, *Angew. Chem., Int. Ed.*, 2018, **57**, 2692–2696; Z.-Y. Liu, M. Zhang and X.-C. Wang, *J. Am. Chem. Soc.*, 2020, **142**, 581–588.
16 (*a*) C. Chen, F. Eweiner, B. Wibbeling, R. Fröhlich, S. Senda, Y. Ohki, K. Tatsumi, S. Grimme, G. Kehr and G. Erker, *Chem.–Asian J.*, 2010, **5**, 2199–2208; (*b*) C. Chen, G. Kehr, R. Fröhlich and G. Erker, *J. Am. Chem. Soc.*, 2010, **132**, 13594–13595; (*c*) C. Chen, T. Voss, G. Kehr, R. Fröhlich and G. Erker, *Org. Lett.*, 2011, **13**, 62–65; (*d*) G. Kehr and G. Erker, *Chem. Commun.*, 2012, **48**, 1839–1850; (*e*) G. Kehr and G. Erker, *Chem. Sci.*, 2016, **7**, 56–65.
17 A. Bismuto, G. S. Nichol, F. Duarte, M. J. Cowley and S. P. Thomas, *Angew. Chem., Int. Ed.*, 2020, **59**, 12731–12735.
18 Although borane-catalyzed hydrosilylation of internal alkynes is known, its application in the hydrosilylation of terminal alkynes has not been disclosed. For the hydrosilylation of internal alkynes with the borane/silane system, see: (*a*) L. D. Curless and M. J. Ingleson, *Organometallics*, 2014, **33**, 7241–7246; (*b*) Y. Kim, B. Ramesh, R. B. Dateer and S. Chang, *Org. Lett.*, 2017, **19**, 190–193; (*c*) X. Zhao, D. Yang, Y. Zhang, B. Wang and J. Qu, *Org. Lett.*, 2020, **22**, 970–975.
19 For computational analysis, see: K. Sakata and H. Fujimoto, *J. Org. Chem.*, 2013, **78**, 12505–12512.
20 Lewis acids, such as $AlCl_3$ and $EtAlCl_2$, which were used in the hydrosilylation of alkynes to produce vinylsilanes, see: T. Sudo, N. Asao, V. Gevorgyan and Y. Yamamoto, *J. Org. Chem.*, 1999, **64**, 2494–2499. However, $AlCl_3$ did not produce 1,1-bis(silane) **4aac** using a combination of $EtMe_2SiH$ and $PhSiH_3$.
21 For air- or moisture-tolerant borane Lewis acid-catalyzed reactions, see: (*a*) K. Ishihara, N. Hanaki, M. Funahashi, M. Miyata and H. Yamamoto, *Bull. Chem. Soc. Jpn.*, 1995, **68**, 1721–1730; (*b*) V. Fasano, J. E. Radcliffe, A. Gyömöre, M. Bakos, T. Földes, I. Pápai, A. Domján and T. Soós, *ACS Catal.*, 2015, **5**, 5366–5372; (*c*) D. J. Scott, T. R. Simmons, E. J. Lawrence, G. G. Wildgoose, M. J. Fuchter and A. E. Ashley, *ACS Catal.*, 2015, **5**, 5540–5544; (*d*) V. Fasano, J. E. Radcliffe and M. J. Ingleson, *ACS Catal.*, 2016, **6**, 1793–1798.
22 (*a*) H. Mayr and G. Hagen, *J. Chem. Soc., Chem. Commun.*, 1989, 91–92; (*b*) M. Horn, L. H. Schappele, G. Lang-Wittkowski, H. Mayr and A. R. Ofial, *Chem. -Eur. J.*, 2013, **19**, 249–263.
23 (*a*) Y. Zhao and D. G. Truhlar, *Theor. Chem. Acc.*, 2008, **120**, 215–241; (*b*) Y. Zhao and D. G. Truhlar, *Acc. Chem. Res.*, 2008, **41**, 157–167.
24 J. Tomasi and M. Persico, *Chem. Rev.*, 1994, **94**, 2027–2094.
25 C. Y. Legault, *CYLview, 1.0b*, Universitéde Sherbrooke, 2009, http://www.cylview.org.
26 Morandi *et al* elegantly proved that the type of silane is also critical to the regioselective deoxygenation of 1,2-Diols, see:

(*a*) N. Drosos and B. Morandi, *Angew. Chem., Int. Ed.*, 2015, **54**, 8814–8818; (*b*) G.-J. Cheng, N. Drosos, B. Morandi and W. Thiel, *ACS Catal.*, 2018, **8**, 1697–1702.

27 L. Wu, S. S. Chitnis, H. Jiao, V. T. Annibale and I. Manners, *J. Am. Chem. Soc.*, 2017, **139**, 16780–16790.

28 H. Mayr, N. Basso and G. Hagen, *J. Am. Chem. Soc.*, 1992, **114**, 3060–3066.

29 J. Bigeleisen and M. G. Mayer, *J. Chem. Phys.*, 1947, **15**, 261–267.

30 (*a*) D. J. O'Leary, P. R. Rablen and M. P. Meyer, *Angew. Chem., Int. Ed.*, 2011, **50**, 2564–2567; (*b*) A. Fong, M. P. Meyer and D. J. O'Leary, *Molecules*, 2013, **18**, 2281–2296.

31 Quantum mechanical tunneling effects were also considered for both methods using the one-dimensional parabolic approximation. (*a*) R. P. Bell, *Chem. Soc. Rev.*, 1974, **3**, 513–544; (*b*) R. P. Bell, *The Tunnel Effect in Chemistry*; Chapman and Hall: New York, 1980; (*c*) D. B. Northrop, *J. Am. Chem. Soc.*, 1999, **121**, 3521–3524.